THE JOURNAL OF BIOLOGICAL CHEMISTRY VOL. 291, NO. 26, pp. 13762–13770, June 24, 2016

Fluorescence Resonance Energy Transfer-based Structural Analysis of the Dihydropyridine Receptor α_{1S} Subunit Reveals Conformational Differences Induced by Binding of the β_{1a} Subunit*

Received for publication, November 25, 2015, and in revised form, April 22, 2016 Published, JBC Papers in Press, April 25, 2016, DOI 10.1074/jbc.M115.704049

Mohana Mahalingam, Claudio F. Perez[1], and James D. Fessenden[2]

From the Department of Anesthesia, Perioperative and Pain Medicine, Brigham and Women's Hospital, Boston, Massachusetts 02115

The skeletal muscle dihydropyridine receptor α_{1S} subunit plays a key role in skeletal muscle excitation-contraction coupling by sensing membrane voltage changes and then triggering intracellular calcium release. The cytoplasmic loops connecting four homologous α_{1S} structural domains have diverse functions, but their structural arrangement is poorly understood. Here, we used a novel FRET-based method to characterize the relative proximity of these intracellular loops in α_{1S} subunits expressed in intact cells. In dysgenic myotubes, energy transfer was observed from an N-terminal-fused YFP to a FRET acceptor, ReAsH (resorufin arsenical hairpin binder), targeted to each α_{1S} intracellular loop, with the highest FRET efficiencies measured to the α_{1S} II-III loop and C-terminal tail. However, in HEK-293T cells, FRET efficiencies from the α_{1S} N terminus to the II-III and III-IV loops and the C-terminal tail were significantly lower, thus suggesting that these loop structures are influenced by the cellular microenvironment. The addition of the β_{1a} dihydropyridine receptor subunit enhanced FRET to the II-III loop, thus indicating that β_{1a} binding directly affects II-III loop conformation. This specific structural change required the C-terminal 36 amino acids of β_{1a}, which are essential to support EC coupling. Direct FRET measurements between α_{1S} and β_{1a} confirmed that both wild type and truncated β_{1a} bind similarly to α_{1S}. These results provide new insights into the role of muscle-specific proteins on the structural arrangement of α_{1S} intracellular loops and point to a new conformational effect of the β_{1a} subunit in supporting skeletal muscle excitation-contraction coupling.

In skeletal muscle excitation contraction (EC)[3] coupling, the dihydropyridine receptor (DHPR), an L-type voltage-gated Ca^{2+} channel, senses membrane depolarization and then initiates intracellular Ca^{2+} release by activating the type 1 ryanodine receptor (RyR1) embedded in the sarcoplasmic reticulum membrane. Of the five skeletal DHPR subunits, α_{1S} and β_{1a} are absolutely required for skeletal type EC coupling (1–8). The 170-kDa α_{1S} subunit contains both the voltage sensor and Ca^{2+} conduction pore and is composed of four homologous domains, each containing six transmembrane segments (9, 10). These domains are connected by intracellular loops with well defined functions. For example the I-II loop has an α_{1S} subunit interaction domain binding site for the β_{1a} DHPR subunit (11, 12), whereas the II-III loop contains an essential determinant (amino acids 720–765) required to activate RyR1 during skeletal-type EC coupling (13, 14). Although the III-IV loop does not appear to have a direct role in RyR1 activation, a malignant hyperthermia mutation located in this loop (R1086H) has been reported to alter DHPR gating properties and EC coupling (15). Finally, the C-terminal tail has been implicated as binding Ca^{2+}/calmodulin (16) as well as mediating proper DHPR targeting to triad junctions (17). Although a recent high resolution cryo-EM reconstruction of the DHPR has resolved many of the membrane-spanning helices in the complex (18), these key α_{1S} intracellular loops are completely absent from the structure, most likely due to intrinsic flexibility. Thus, understanding the relative arrangement of these loops as well as how they change conformation due to binding of cell-specific factors remain as key questions.

Like the α_{1S} subunit, the β_{1a} DHPR subunit also plays an essential role in skeletal muscle EC coupling. β_{1a} is required to target α_{1S} to the cell surface and to support depolarization-induced intracellular Ca^{2+} release (*i.e.* orthograde signaling) as well as to enhance DHPR inward Ca^{2+} current (*i.e.* retrograde signaling) (2, 5, 19). β_{1a} is also needed to assemble the DHPR complex into tetradic arrays visualized in freeze-fracture studies (20–22). An essential determinant between residues 489–503 of the β_{1a} C-terminal tail is required for both bidirectional signaling and tetrad formation (22, 23).

Recent structural analysis of the DHPR intracellular loops has been achieved using fluorescence resonance energy transfer (FRET) measurements between cyan and yellow fluorescent proteins (CFP/YFP) fused into α_{1S} and β_{1a} (24, 25). These studies have suggested a direct role of RyR1 in the structural organization of the α_{1S} subunit and have identified potential RyR-

* This work was supported by National Institutes of Health Grants R03AR066359 (to C. F. P.), R01AR059124 (to J. D. F.), and R01AR067738 (to C. F. P. and J. D. F.). The content is solely the responsibility of the authors and does not necessarily represent the official views of the National Institutes of Health. The authors declare that they have no conflicts of interest with the contents of this article.

[1] To whom correspondence may be addressed: Brigham and Women's Hospital, 75 Francis St., Boston MA 02115. Tel.: 617-525-6486; Fax: 617-732-6927; Email: cperez@zeus.bwh.harvard.edu.

[2] To whom correspondence may be addressed: Brigham and Women's Hospital, 75 Francis St., Boston MA 02115. Tel.: 617-525-8332; Fax: 617-732-6927; E-mail: jfessenden@zeus.bwh.harvard.edu.

[3] The abbreviations used are: EC, excitation-contraction; DHPR, dihydropyridine receptor; RyR, ryanodine receptor; CFP, cyan fluorescent protein; ReAsH, resorufin arsenical hairpin binder; Tc, tetracysteine; FRET, fluorescence resonance energy transfer; YFP, yellow fluorescent protein.

interacting domains in α_{1S} and β_{1a}. Although these studies illustrate the potential of FRET-based approaches for structural analysis of the DHPR complex *in situ*, they have been hampered by the relative bulkiness of the fused CFP/YFP FRET probes, as suggested by functional impairments of α_{1S} subunits carrying a fluorescent protein fused into the III-IV loop (25). In addition, FRET data derived exclusively from fluorescent protein insertions can be difficult to interpret due to the distance between their chromophoric centers and their insertion sites (26) as well as the bulkiness of these inserted proteins.

In this report we used an innovative site-specific labeling method combined with FRET-based structural measurements to determine the spatial interrelationships between cytoplasmic loops of α_{1S} subunits expressed in cultured myotubes harboring the α_{1s} muscular dysgenesis mutation (*mdg*) (6, 7), which renders these dysgenic myotubes completely deficient in native α_{ls} expression (6). Energy transfer was measured from YFP fused to the N terminus of α_{1s} to the cell-permeant resorufin arsenical hairpin binder ReAsH (27) targeted to short tetracysteine (Tc) motifs inserted into each of the α_{1S} intracellular loops. Our results suggest that within the triadic environment, the α_{1s} loops are clustered together, with the II-III loop and C terminus being closest to the α_{1S} N terminus. However, in a non-myogenic system (HEK-293T cells), FRET to the II-III and III-IV loops and the C-terminal tail is significantly lower, thus suggesting that cellular microenvironment influences α_{1S} structure. Finally, we found that binding of the β_{1a} subunit affects the structure of the α_{1S} II-III loop *in situ*. This study reveals the influence of muscle-specific environmental factors on the arrangement of the α_{1S} cytosolic loops and provides the first direct evidence that the β_{1a} subunit modulates the α_{1S} II-III loop conformation.

Experimental Procedures

α_{1S} DHPR cDNA Cloning—A full-length rabbit α_{1S} cDNA (amino acids 1–1873) (GenBank™ accession number M23919) was cloned in-frame downstream from the YFP-citrine gene (28) in the bicistronic retroviral vector pCMMP-MCS-IRES-Puro, containing a puromycin resistance gene (Addgene 36952; Ref. 29). Insertion of a Tc tag-encoding sequence (FLNCCPGCCMEP) into α_{1S} was performed using Gibson assembly (New England BioLabs). Double-stranded DNA fragments (*i.e.* gBlocks, Integrated DNA Technologies) encoding the Tc tag were inserted in-frame at the following α_{1S} locations; I-II loop (amino acid 388), II-III loop (amino acid 719 and 726), III-IV loop (amino acid 1076), and C-terminal tail (amino acid 1636). A Tc tag at the N-terminal end (amino acid 1) was inserted in-frame upstream of the YFP sequence as a positive control in FRET experiments, and all clones were confirmed by DNA sequencing.

β_{1a} DHPR cDNA Cloning and Purification—Full-length mouse β_{1a} cDNA (GenBank™, NM_031173) was cloned into the pCold-II expression vector (Takara™) in-frame downstream from a streptavidin binding tag, which was used to assist with purification. The clone was expressed in the *Escherichia coli* BL21 strain in combination with the pG-KJE8 vector (Takara™) to optimize protein folding. Protein induction and purification were performed using isopropyl 1-thio-β-D-galactopyranoside/arabinose/tetracycline and Strep-trap affinity chromatography columns as described (30).

Cell Culture and Immunocytochemistry—cDNAs were expressed in dysgenic myotubes after packaging into lentivirus using a set of three packaging vectors as described (22). Dysgenic myoblasts were infected with lentiviral particles containing YFP-α_{1S} cDNAs at a multiplicity of infection = 0.5 and then selected with 1.5 μg/ml puromycin for 2 weeks. Individual myoblast colonies stably transduced with each clone were then isolated using glass rings.

DHPR-expressing myoblasts were grown and differentiated in 96-well plates as described (22). α_{1S} DHPR expression was confirmed by immunocytochemistry on methanol-fixed cultured myotubes using either anti-α_{1S} MA3–921 (Thermo Scientific) or anti-GFP G10362 (Life Technologies) monoclonal antibodies.

HEK-293T cells were grown and polyethyleneimine-transfected with Tc-tagged YFP-α_{1S} cDNAs as described (31). Two days after transfection, cells were tested in FRET-based assays.

Calcium Imaging—After differentiation for 4–5 days, myotubes expressing YFP-α_{1S} cDNAs were loaded with 5 μM Fura-2 AM (Molecular Probes) in imaging buffer (125 mM NaCl, 5 mM KCl, 2 mM $CaCl_2$, 1.2 mM $MgSO_4$, 6 mM glucose, and 25 mM HEPES/Tris, pH 7.4). Membrane depolarization was performed by a 5-s perfusion with 5–7 volumes of imaging buffer containing increasing concentrations of KCl. Cells were imaged with an intensified 10-bit digital CCD camera (XR-Mega-10, Stanford Photonics, Stanford, CA) using a DG4 multiwavelength light source (Sutter Instruments, Novato, CA). Fluorescent emission at 510 nm was captured from regions of interest within each myotube at 33 frames per second using Piper acquisition software (Stanford Photonics) and expressed as ratio of signal collected at alternating 340/380-nm excitation wavelengths. Calcium transients quantified from the peak amplitudes were plotted as a function of added KCl and fit to a sigmoidal dose-response function (variable slope) to determine EC_{50} values, which were then compared via analysis of variance.

Labeling with FRET Acceptors—ReAsH labeling of Tc-tagged α_{1S}- expressing intact cells was performed as described (32) with some modifications. ReAsH was first complexed with ethane dithiol (EDT) for 10 min in a reaction consisting of 0.5 mM ReAsH and 12.5 mM EDT in DMSO. This reaction mixture was diluted 1:1000 in FRET buffer consisting of 125 mM NaCl, 5 mM KCl, 6 mM glucose, and 25 mM HEPES, pH 7.6, and then added to myotubes or HEK-293T cells expressing Tc-tagged YFP-α_{1S} constructs. Cells were incubated at 37 °C for 1.5 h followed by washing with 100 μM British anti-Lewisite for 15 min to reduce nonspecific ReAsH labeling. In some experiments HEK-293T cells expressing Tc-tagged YFP-α_{1S} constructs were permeabilized with 0.1% saponin and then incubated with 150 nM purified β_{1a} protein for 2 h at 37C. Cells were then tested in FRET experiments (see below).

FRET measurements between α_{1S} and β_{1a} subunit were conducted using the His-tag-specific FRET acceptor, Cy3NTA, as described previously (31). HEK-293T cells expressing YFP-α_{1S} constructs were permeabilized using 0.1% saponin in FRET buffer containing 3 μM Cy3NTA with or without 150 nM purified β_{1a} protein bearing 10 histidine residues (His_{10}) at its

N-terminal end. After incubation for 2 h at 37 C, cells were analyzed for FRET.

FRET Imaging—FRET was measured using epifluorescence microscopy as described (31, 33). Briefly, YFP donor fluorescence was acquired using a 480/30-nm bandpass excitation filter and 535/40-nm bandpass emission filter as a series of 60 16-bit 672 × 516 pixel images across a z stack 60 μm in thickness. Acceptor fluorescence was photobleached for 4 min at maximum DG-4 light source intensity using a ReAsH cubeset composed of a 570/20-nm bandpass excitation filter and 620/60-nm bandpass emission filter. FRET was measured as an enhancement in donor fluorescence upon acceptor photobleaching using,

$$E = 1 - (F_{\text{prebleach}}/F_{\text{postbleach}}) \quad \text{(Eq. 1)}$$

where E represents FRET efficiency, and $F_{\text{prebleach}}$ and $F_{\text{postbleach}}$ indicate donor fluorescence intensities before and after acceptor photobleaching, respectively. Fluorescence was quantified using ImageJ version 1.43u as described (34).

Measurement of ReAsH Labeling Efficiency—For each Tc-tagged YFP-α_{1s} construct expressed in HEK-293T cells, YFP and ReAsH fluorescence was quantified both before and after ReAsH photobleaching. ReAsH labeling efficiency was then calculated as the ratio of ReAsH (pre-acceptor bleach) to YFP (post-acceptor bleach) fluorescence for each construct. Note that YFP fluorescence acquired after acceptor bleach was used for these calculations to eliminate any contribution of YFP/ReAsH FRET from these measurements.

Molecular Visualization and Distance Measurements—An atomic model (Protein Data Bank Accession code 3JBR) derived from a high resolution cryo-EM reconstruction of the full DHPR complex (18) was used for distance measurements and preparation of Fig. 7, which was created using Chimera image processing software version 1.10.1 (build 40427) (35).

Results

Expression and Functional Analysis of Tc-tagged YFP-α_{1S} DHPRs in Dysgenic Myotubes—To characterize the relative proximity of the cytoplasmic loops in the α_{1S} DHPR subunit using FRET, we fused citrine, a bright YFP variant (28), to the N terminus of α_{1S} to act as a FRET donor. Then we inserted short Tc motifs (FLNCCPGCCMEP; Ref. 27) separately into each α_{1S} cytoplasmic loop and domain (Fig. 1*A*) to act as binding sites for the FRET acceptor ReAsH. Proper targeting of these Tc-tagged YFP-α_{1S} fusion constructs to the junctional sarcoplasmic reticulum of stably transduced dysgenic myotubes was confirmed by immunocytochemistry (Fig. 1*B*). After staining with an anti-GFP antibody, both YFP-α_{1S} and Tc-tagged YFP-α_{1S} constructs displayed discrete fluorescent foci that closely resembled the immunofluorescent pattern observed in wild type myotubes labeled with anti-α_{1S} antibodies (Fig. 1*B*). This staining pattern is known to represent the peripheral couplings where the sarcoplasmic reticulum terminal cisternae interact with the surface membrane (36). These results suggest that Tc-tag insertions did not affect α_{1S} targeting to peripheral couplings.

To functionally characterize these Tc-tagged α_{1S} channels, we quantified depolarization-induced Ca^{2+} release (*i.e.* EC coupling) in Fura-2-loaded stably transduced dysgenic myotubes. Each Tc-tagged α_{1S} construct restored robust Ca^{2+} release in response to K^+-depolarization. This Ca^{2+} release was comparable with control myotubes expressing YFP-α_{1S} lacking a Tc tag (−*Tc*; Fig. 2*A*). A small but significant reduction in average peak Ca^{2+} transient was observed in myotubes expressing constructs Tc-tagged at the N terminus, I-II loop, and II-III loop (Fig. 2*B*). Because no changes in sensitivity to K^+ depolarization were observed for these constructs compared with −Tc controls ($p > 0.05$), it is conceivable that the smaller Ca^{2+} transients result from slight differences in α_{1S} expression between individual cell clones. Myotubes expressing a Tc-tagged III-IV loop α_{1S} construct restored robust EC coupling though with enhanced K^+ sensitivity. Mutations in the III-IV loop region have been reported to affect the conductive properties of the α_{1S} subunit (15, 37). However, whether the insertion of the Tc tag in our study alters the voltage-sensing properties of the DHPR complex is currently unknown and will require further testing. Thus, even though small functional changes were observed in some cases, the overall targeting and function of these YFP-α_{1S} constructs was largely unaffected by the Tc-tag insertions.

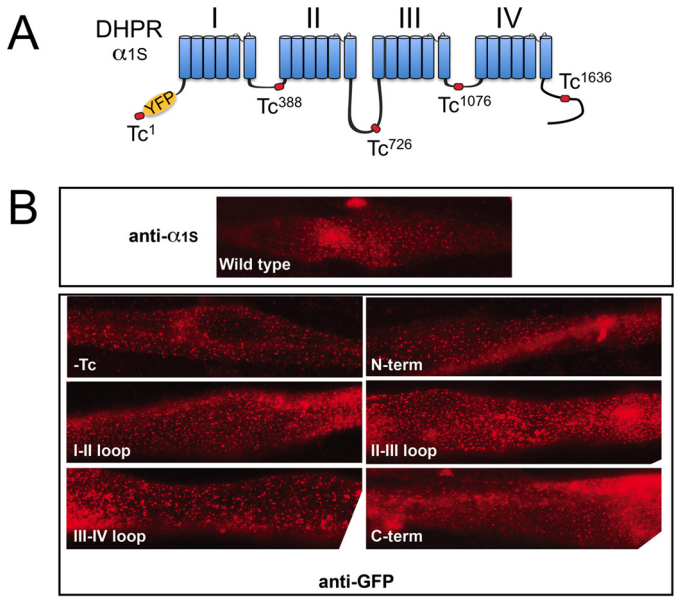

FIGURE 1. **Tc-tagged YFP-α_{1S} DHPR fusion proteins are efficiently targeted to peripheral couplings in dysgenic myotubes.** *A*, schematic representation of the α_{1S} DHPR subunit. YFP (*yellow oval*) and α_{1S} protein sequence positions of the Tc tag insertions in each intracellular loop and domain are shown. *B*, representative immunolocalizations of Tc-tagged YFP-α_{1S} constructs stably expressed in dysgenic myotubes. Punctate localization pattern for these recombinant constructs probed with an anti-GFP antibody (*bottom panels*) is similar to immunostaining pattern for wild type myotubes labeled with an anti-α_{1S} antibody (*top panel*).

FRET-based Structural Analysis of Tc-tagged YFP-α_{1S} DHPRs—FRET-based analysis was used to characterize the structural arrangement of the α_{1S} intracellular loops (Fig. 3). The cell-permeant biarsenical FRET acceptor, ReAsH (27), was targeted to the Tc-tagged YFP-α_{1S} constructs (Fig. 3*A*), and energy transfer was quantified from the increase in the N-terminally fused YFP donor fluorescence after acceptor photobleaching (34). As reported (38), untransfected dysgenic myotubes were strongly labeled by ReAsH, which persisted even

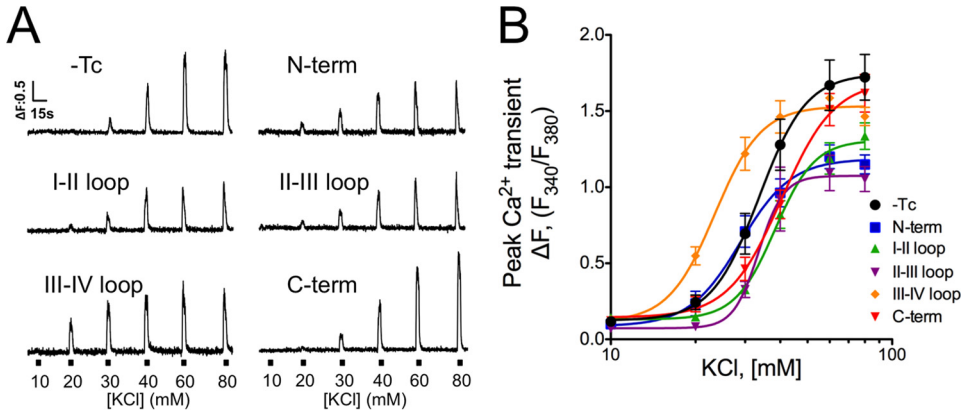

FIGURE 2. **Tc-tagged YFP-α_{1S} DHPRs restore depolarization-induced calcium release in dysgenic myotubes.** *A*, representative fluorescent traces of K^+-induced Ca^{2+} release responses of dysgenic myotubes stably transduced with the indicated YFP-α_{1S} constructs. Myotubes loaded with 5 μM Fura-2 were exposed to increasing concentrations of KCl for 5 s (*black boxes*). *B*, average peak Ca^{2+} transient amplitude of control (−Tc) and Tc-tagged α_{1S} constructs expressed in dysgenic myotubes. Note that the II-III loop construct was tested in transiently transfected myotubes. The data are from 2 experiments (10–25 cells total) and are presented as the mean ± S.E.

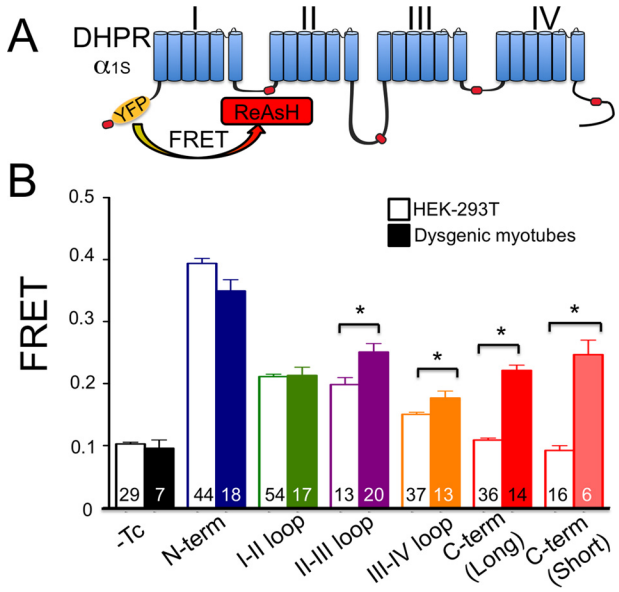

FIGURE 3. **FRET-based structural measurements of the α_{1S} DHPR subunit reveal key conformational differences caused by the cellular microenvironment.** *A*, schematic representation of the FRET donor/acceptor pair in the α_{1S} DHPR subunit. YFP (*yellow oval*) acts as a FRET donor, transferring energy to the FRET acceptor ReAsH, targeted specifically to tetracysteine tags (*red rectangles*) separately inserted into each α_{1S} cytoplasmic loop. *B*, FRET efficiency values are shown from the N-terminal YFP to ReAsH targeted to the indicated α_{1S} intracellular loops for constructs expressed in either HEK-293T cells (*open bars*) or dysgenic myotubes (*filled bars*). Data points represent mean FRET efficiency values ± S.E. for the number of cells indicated in each *bar*. The *asterisk* indicates a significant difference in energy transfer ($p < 0.01$ using a paired two-tailed *t* test) for a given construct tested in either HEK-293T cells or dysgenic myotubes. *Short* and *Long C-term* constructs contain a Tc tag at position 1636 and a stop codon inserted at either position 1664 or 1873, respectively. All other constructs are full-length (*i.e.* 1873 residues).

after washing with British anti-Lewisite (39) to remove nonspecific ReAsH labeling (data not shown). However, this background ReAsH labeling did not impede our ability to measure FRET as only very low background energy transfer ($E = 0.1$) was observed in ReAsH-labeled myotubes expressing non-Tc-tagged control YFP-α_{1S} (−Tc). On the other hand, significant energy transfer above background was detected to ReAsH separately targeted to each intracellular domain (Fig. 3*B*, *filled bars*). As expected, a positive control construct consisting of a Tc-tag/YFP tandem fused at the α_{1S} N terminus displayed the highest FRET efficiency (*N-term*, $E = 0.35$; Fig. 3*B*), similar to FRET values previously reported for this same tandem inserted into RyR1 (34). FRET efficiencies measured to the I-II loop ($E = 0.20$), II-III loop ($E = 0.25$), and the C-terminal tail ($E = 0.24$) were also significantly higher compared with the −Tc negative control construct. Average FRET efficiency measured to the III-IV loop ($E = 0.18$) was slightly but significantly reduced compared with the II-III loop and C-terminal domain ($p < 0.05$), thus suggesting differences among the loops in either relative distance to the α_{1S} N terminus and/or orientation of the Tc tags. Overall, these results indicate that FRET efficiencies measured between the α_{1S} N terminus and each cytoplasmic domain are similar, and therefore, these loops might be tightly clustered in dysgenic myotubes.

Previous FRET studies have suggested that skeletal muscle-specific protein-protein interactions can affect the organization of the α_{1S} cytoplasmic loops (25). Thus, we performed a parallel series of FRET measurements on these α_{1S} constructs expressed in HEK-293T cells (Fig. 3*B*, *open bars*), which lack skeletal muscle-specific proteins including the DHPR and RyR1. ReAsH-labeled HEK-293T cells expressing YFP-α_{1S} (*−Tc*) displayed background energy transfer ($E = 0.10$) unchanged compared with FRET measurements for this construct expressed in dysgenic myotubes (Fig. 3*B*, *black bars*). Similarly, FRET efficiencies measured in HEK-293T cells to ReAsH targeted to the α_{1S} N terminus and I-II loop ($E = 0.39$, and $E = 0.21$, respectively) were unchanged compared with similar measurements conducted in dysgenic myotubes. However, in intact HEK-293T cells, average FRET efficiencies to the II-III loop ($E = 0.20$) and III-IV loop ($E = 0.14$) were significantly reduced compared with measurements in dysgenic myotubes (Fig. 3*B*). Most surprisingly, no significant energy transfer above background was detected to the α_{1S} C-terminal tail in HEK-293T cells ($E = 0.10$) despite robust FRET to this position for measurements conducted in dysgenic myotubes. This striking difference in energy transfer was unrelated to myotube-specific post-translational cleavage of the C-terminal tail at position 1664. As shown in Fig. 3*B*, FRET efficiencies measured from HEK-293T cells expressing α_{1s} containing a full-length

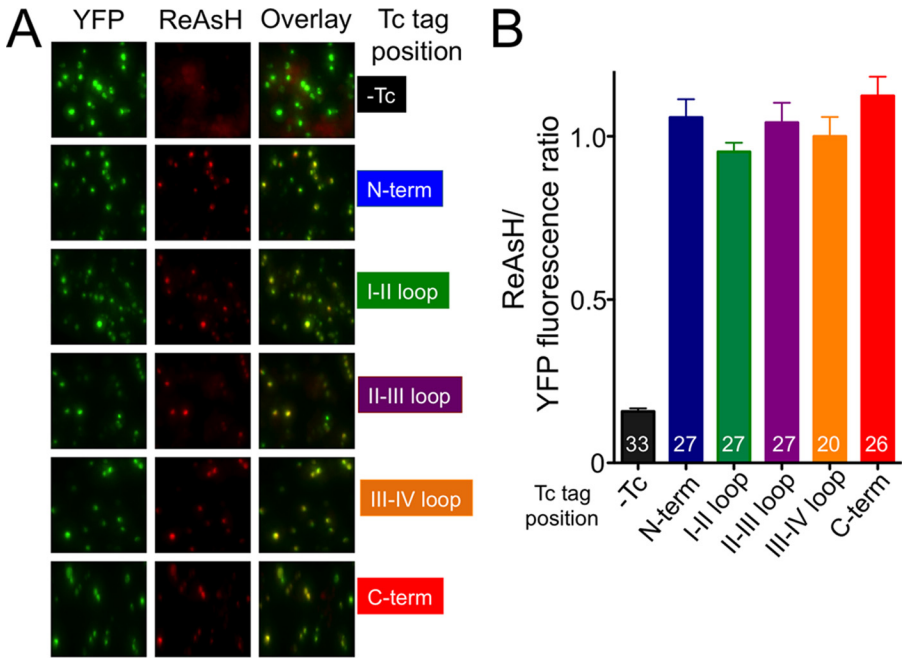

FIGURE 4. **The ReAsH FRET acceptor is targeted with equal efficiency to all α_{1S} cytoplasmic loop positions.** *A*, representative images of HEK-293T cells expressing ReAsH-labeled Tc-tagged YFP-α_{1S} DHPR constructs monitored for YFP (*left panels*) and ReAsH fluorescence (*middle panels*) as well as the overlay between the two signals (*right panels*). Significant signal overlap was observed for all constructs except YFP-α_{1S}, lacking a Tc tag (*top panels*). *B*, ReAsH labeling efficiency is shown for all constructs as the ratio of ReAsH/YFP fluorescence. Values represent the mean ± S.E. for the number of cells indicated in each bar. No significant differences in ReAsH labeling efficiency were noted between the Tc-tagged constructs ($p > 0.05$ using analysis of variance).

C-terminal tail were not different from those measured in cells expressing the C-terminal tail truncated at position 1668. Thus, these results suggest that the conformation of the α_{1S} II-III and III-IV loops and particularly the C-terminal tail are influenced by the cellular microenvironment.

ReAsH Labeling Efficiency—To verify that differences in energy transfer observed between the various Tc-tagged α_{1S} constructs were not due to differences in ReAsH labeling efficiency at the various Tc-tagged sites, we quantified ReAsH labeling to each construct expressed in HEK-293T cells (Fig. 4). In contrast to dysgenic myotubes, specific ReAsH labeling of each recombinant Tc-tagged α_{1S} DHPR was readily observed after treatment with 100 μM British anti-Lewisite (Fig. 4*A*), as we have shown previously with Tc-tagged RyRs expressed in HEK-293T cells (34). However, no differences in ReAsH labeling efficiency (*i.e.* the ReAsH/YFP fluorescence ratio) were observed between the Tc-tagged YFP-α_{1S} constructs (Fig. 4*B*). Because of high nonspecific ReAsH labeling in myotubes, these control experiments were not feasible. However, in these cells FRET efficiencies measured after labeling Tc-tagged α_{1S} YFP constructs with either 0.5 μM ReAsH (*i.e.* the concentration used in all FRET experiments) or a 4-fold higher ReAsH concentration (2 μM) were identical (data not shown), thus indicating that 0.5 μM ReAsH is a saturating concentration for these measurements. These results indicate that, as in HEK-293T cells, differences in FRET efficiencies measured in dysgenic myotubes does not result from trivial differences in ReAsH accessibility.

Effect of β_{1a} Binding on α_{1S} Loop Structure—The β_{1a} DHPR subunit is critical for α_{1S} membrane targeting and Ca^{2+} channel function as well as EC coupling (2, 4, 5, 22). To determine whether this essential subunit was responsible for differences in energy transfer observed in the two cell expression systems, we assessed the effect of direct addition of exogenous β_{1a} subunit on FRET efficiencies measured in HEK-293T cells. For these experiments, saponin-permeabilized cells were incubated with and without 150 nM purified recombinant β_{1a} subunit, which saturates α_{1S} expressed in HEK-293T cells (data not shown). In the absence of β_{1a}, measured energy transfer to each α_{1S} cytoplasmic loop in permeabilized HEK-293T cells (Fig. 5*B*, *open bars*) was comparable to similar measurements in intact HEK-293T cells (Fig. 3*B*, *open bars*), suggesting that cell permeabilization did not significantly affect the structure of the cytosolic loops/domains. Upon incubation with β_{1a} (Fig. 5*B*, *filled bars*) no significant changes in energy transfer were observed to any position except the II-III loop, where β_{1a} addition significantly increased FRET efficiency from 0.22 to 0.30 ($p < 0.05$). This finding was confirmed using a second II-III loop Tc-tagged construct (at position 719), where β_{1a} enhanced FRET from 0.26 to 0.31 (Fig. 5*B*). Recombinant β_{1a} lacking its C-terminal 36 amino acids (β_{-36}), which are required to support bidirectional signaling (9), did not enhance FRET from the N-terminal YFP to the II-III loop (Fig. 5*B*, *gray bar*), thus indicating that these C-terminal tail residues are required to mediate β_{1a}-induced conformational changes in the α_{1S} II-III loop.

β_{1a} binding specificity was confirmed using a YFP-α_{1S} Tc-tagged II-III loop construct harboring a Y366S mutation, which disrupts β_{1a} binding to the α_{1S} subunit interaction domain motif in the α_{1S} I-II loop (11). This Y366S α_{1S} mutation completely prevented β_{1a}-mediated enhancement in FRET to the II-III loop (Fig. 5*C*), thus confirming that β_{1a} binding to its native α_{1S} subunit interacting domain motif is required for its conformational effects on the II-III loop.

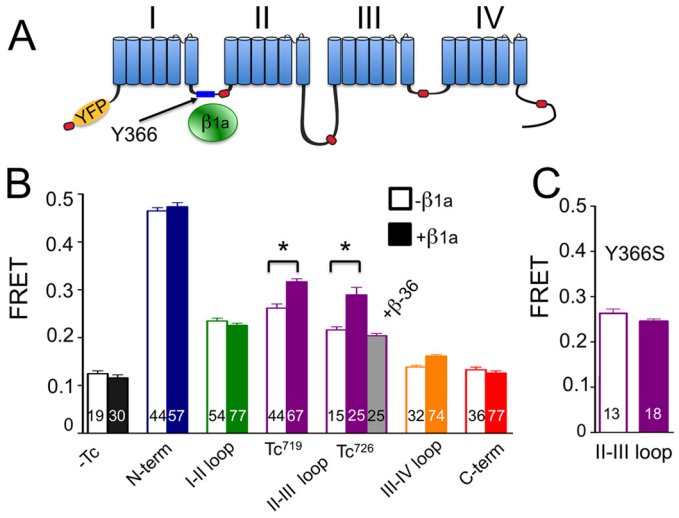

FIGURE 5. **The β_{1a} DHPR subunit specifically alters the structure of the α_{1S} II-III loop.** *A*, schematic representation of the α_{1S} DHPR subunit showing the position of YFP (*yellow oval*), Tc tags (*red squares*), and the β_{1a} DHPR subunit (*green oval*) bound to its α_{1S} subunit interacting domain determinant in the I-II loop (*blue rectangle*). The location of the critical Y366 residue required for β_{1a} binding to α_{1S} is shown. *B*, average FRET efficiency values are shown from YFP in the α_{1S} N terminus to ReAsH targeted to permeabilized HEK-293T cells expressing the indicated Tc-tagged α_{1S} DHPR constructs in either the absence (*open bars*) or presence (*filled bars*) of 150 nM recombinant β_{1a}. The effect of β_{1a} lacking 36 C-terminal amino acids (β-36) on FRET efficiency to the II-III loop is shown (*gray bar*). Data points represent mean FRET efficiencies ± S.E. for the number of cells indicated in each bar. *Asterisks* indicate a significant difference in energy transfer ($p < 0.01$ using a paired two-tailed *t* test) between FRET measurements for a given construct conducted in either the absence or presence of β_{1a}. *C*, average FRET efficiency values are shown from YFP in the N terminus of α_{1S} to ReAsH targeted to Tc726 in the II-III loop of α_{1S} containing the Y366S mutation, which cannot bind β_{1a} (11). Data points represent mean FRET efficiencies ± S.E. for the number of cells indicated in each *bar*.

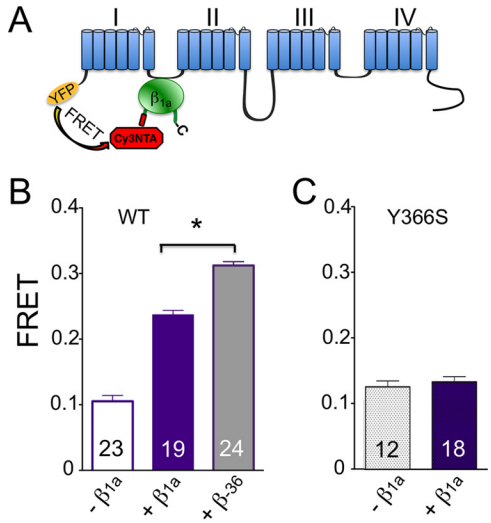

FIGURE 6. **Both β_{1a} and β-36 bind to α_{1S} DHPR.** *A*, strategy for direct FRET measurements between α_{1S} and β_{1a} DHPR subunits in HEK-293T cells. FRET from the fused N-terminal YFP in α_{1S} (*yellow oval*) to the His_{10} tag-specific FRET acceptor, Cy3NTA (*red octagon*), targeted to β_{1a} (*green circle*) is indicative of binding between these two DHPR subunits. *B* and *C*, FRET efficiency values are shown from YFP to Cy3NTA targeted to HEK-293T cells expressing wild type YFP α_{1S} (*B*) or Y366S YFP α_{1S} (*C*) with and without the indicated β_{1a} constructs. Data represent the mean FRET values ± S.E. for the number of cells indicated in each *bar*. The *asterisk* indicates a significant difference in energy transfer ($p < 0.001$ using a paired two-tailed *t* test) between FRET measurements conducted using either wild type β_{1a} or truncated β-36.

FRET between α_{1S} and β_{1a}—Direct binding of both wild type and truncated β_{1a} to α_{1S} in HEK-293T cells was confirmed by measuring FRET from the N-terminal-fused YFP of α_{1S} to the FRET acceptor Cy3NTA (31) targeted to a His_{10} tag attached to the β_{1a} N terminus (Fig. 6*A*). Significant energy transfer was observed after incubation with β_{1a} subunit ($E = 0.24$) compared with background ($E = 0.10$). Incubation with truncated β_{-36} resulted in an even greater increase in energy transfer ($E = 0.31$), significantly higher than FRET measured with wild type β_{1a} (Fig. 6*B*), thus suggesting that deletion of the β_{1a} C terminus may affect the relative α_{1S}/β_{1a} orientation. This finding is consistent with the suggested role of the β_{1a} C-terminal tail in supporting domain cooperativity within the subunit (40). Binding specificity was confirmed using the Y366S-α_{1S} mutation, which prevented specific energy transfer between α_{1S} and β_{1a} (Fig. 6*C*). These findings indicate that both wild type and truncated β_{1a} bind to the I-II loop of α_{1S} expressed in HEK-293T cells.

Discussion

In this study using a unique FRET-based approach we have shown that the DHPR α_{1S} subunit intracellular loops have remarkably similar structural properties when expressed either in myotubes or HEK-293T cells. However, key differences exist. To our knowledge we are the first to show that the structure of the α_{1S} C-terminal tail is highly sensitive to muscle-specific protein-protein interactions. Our data also provide the first experimental evidence of a β_{1a}-mediated reorientation of the α_{1S} II-III loop domain, further supporting the idea that a synergistic α_{1S}/β_{1a} interaction could account for the conformational changes required to sustain skeletal muscle E-C coupling. The details of these findings and our unique FRET-based experimental system are outlined below.

Labeling System—FRET-based analysis of the DHPR using fused fluorescent proteins as FRET donors/acceptors has become a powerful tool for *in situ* studies of DHPR conformation and its structural interaction(s) with RyR1 (24, 25). Although these studies have revealed important structural aspects of DHPR/RyR interactions, they are limited by the exclusive use of fluorescent proteins, which can affect DHPR function and targeting as well as interpretation of the resulting FRET data (25, 26, 41). In the current study a small 12-residue peptide tag was used to target the FRET acceptor, ReAsH, to each of the α_{1S} DHPR cytoplasmic loops and domains, thereby minimizing alteration of native protein conformation. Thus, we could measure FRET to the α_{1S} III-IV loop without compromising DHPR function or proper targeting, which are both severely disrupted by insertion of larger FRET probes (*i.e.* fluorescent protein fusions) in this loop (25). In addition, we could easily quantify energy transfer to a specific Tc tag via direct comparison with non-−Tc-tagged controls. And because all DHPR loop positions were equally accessible to FRET acceptor, measured FRET efficiencies could more easily be related to differences in either donor/acceptor distance or orientation. Finally, nonspecific biarsenical labeling of myotubes reported previously (38) was not problematic for these studies, as ReAsH was used as FRET acceptor, and so only ReAsH fluorophores tar-

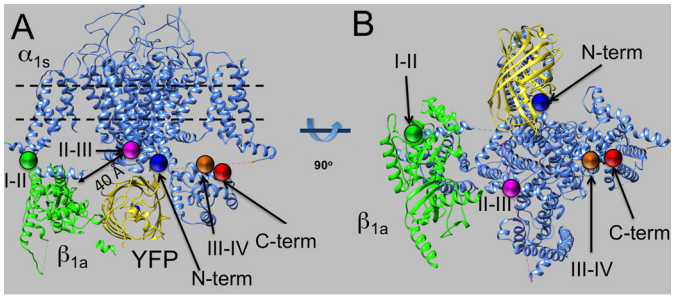

FIGURE 7. **Model of the skeletal muscle DHPR complex.** *A*, structure of the DHPR complex derived from high resolution cryo-EM reconstructions. α_{1S} (*blue*) and β_{1a} (*green*) subunits are shown as well as a putative location of YFP (*yellow*) fused to the α_{1S} N terminus. Locations of the intradomain loops in the α_{1S} subunit are shown as *colored dots* as well as the distance from the center of the II-III loop to the β_{1a} subunit. The plasma membrane lipid bilayer is depicted as *dashed lines*. Structure is shown in cross-section with the extracellular face of the channel at the *top of the figure*. *B*, DHPR complex viewed from the cytoplasmic side after 90° rotation as shown. Note that because intradomain loops are not defined in the high resolution maps, *arrows* point to *colored spheres* arbitrarily placed at the center of a line connecting the nearest known sequence elements flanking each loop.

geted to α_{1S} Tc tags proximal to the fused YFP donor contributed to the measured FRET.

Comparison between Loop Conformations in Heterologous and Homologous Systems—We observed remarkable similarities and differences in the structure of α_{1S} expressed either in HEK-293T cells or dysgenic myotubes. For example, FRET measurements to the N terminus and the I-II loop were essentially identical between the two systems, thus suggesting that cell-specific factors do not affect FRET measured to these areas. In contrast, FRET efficiencies measured from the α_{1S} N terminus to the II-III, III-IV loops and, most significantly, to the C-terminal tail were all quite different between the two systems. We can attribute some of these differences to specific protein factors, whereas other differences will require additional experiments to investigate. A summary of these differences follows.

II-III Loop Structure—Compared with identical measurements in HEK-293T cells, we observed a significant elevation in energy transfer from the N terminus to the α_{1S} II-III loop for constructs expressed in dysgenic myotubes. This increase in FRET likely reflects a specific conformational effect in the II-III loop as structural changes in the vicinity of the N-terminal YFP FRET donor common to all constructs would almost certainly have altered FRET efficiencies to all DHPR loops. This enhanced energy transfer to the II-III loop most likely results from binding of β_{1a} to its I-II loop determinant, as we observed the same degree of elevated energy transfer to the II-III loop in HEK-293T cells incubated with recombinant β_{1a}. Because β_{1a} enhanced FRET to two different Tc-tagged positions in the II-III loop, this effect is reproducible and meaningful. This specific conformational change in the II-III loop also requires the C-terminal 36 amino acids of β_{1a}, a determinant needed to support EC coupling and to organize DHPRs into tetrads (22, 23). This conformational effect might reflect the natural structure of this II-III loop required to communicate with RyR1. Moreover, the II-III loop and the C-terminal tail of β_{1a} might form a larger structural domain that then interacts with RyR1 (a notion supported by recent cryo-EM reconstructions of the DHPR; see Fig. 7*A* below). Although these possibilities require testing, it should be stressed that the only specific conformational effect of β_{1a} binding we observed was within the II-III loop. Future FRET-based measurements to more defined determinants in the II-III loop may resolve more subtle structural changes occurring as a result of β_{1a} binding or during EC coupling.

III-IV Loop Structure—In this study we were able to make the first direct FRET measurements to the III-IV loop. We detected very slight differences in FRET to the III-IV loop when constructs were expressed either in HEK-293T cells or dysgenic myotubes. The origin of these differences is still difficult to discern but appear to be unrelated to β_{1a} binding. However, now that the III-IV loop can be labeled with FRET acceptors, future studies may detect structural changes in this loop that provide clues as to its function.

C-terminal Tail Structure—The largest difference we observed in FRET measurements conducted in the two systems was to the α_{1S} C-terminal tail. Robust FRET was measured to this position when experiments were conducted in myotubes, whereas no significant FRET was detected in HEK-293T cells. These differences suggest changes in structural conformation of the C-terminal tail that could result from post-translational processing of the α_{1S} subunit or differences in protein composition between the two systems as discussed below.

Posttranslational Processing of α_{1S}—Differences in FRET efficiencies measured between the N terminus and the C-terminal tail may result from intrinsic differences in post-translational processing of α_{1S} in dysgenic myotubes. For this study we used an α_{1S} construct encoding the full 1873 amino acids of the protein. However, in myotubes, full-length α_{1S} subunit is likely cleaved post-translationally at position 1664 (25, 42), right after our Tc-tag insertion, thus significantly shortening the C-terminal tail. To test whether post-translational processing of the C-terminal tail may have affected FRET efficiencies measured to this position, we conducted parallel FRET measurements on α_{1s} YFP fusion constructs with either a full-length C-terminal tail or a tail shortened at position 1668. No differences in FRET for these variants were observed in either HEK-293T cells or dysgenic myotubes. Thus, it is unlikely that post-translational processing of the C-terminal tail results in the different FRET efficiency profiles to these different positions.

Muscle-specific Proteins—Differences in FRET efficiency to the C-terminal tail of α_{1S} were significant and unrelated to the absence of β_{1a} subunit in HEK-293T cells. Similarly, differences in interactions with RyR1 most likely are not responsible for changes in FRET to the α_{1S} C terminus, as previous studies using CFP/YFP fusions showed no difference in FRET between the N and C termini for α_{1S} constructs expressed in either dyspedic (*i.e.* lacking RyR1) or dysgenic systems (25). Thus, it is possible that other proteins that make up the DHPR complex, such as the $\alpha_2\delta1$ and $\gamma1$ subunits, might account for this difference. Similarly, interactions between the α_{1S} C terminus tail and other muscle-specific proteins should not be ruled out. Indeed, differences in protein interactions with various functional domains of the α_{1S} C-terminal tail, like the triad targeting signal (position 1543–1661; Refs. 44 and 45) and the AKAP/PKA binding domain (position 1724–1821; Ref. 42) might lead to conformational changes in the C-terminal tail evident in myotubes but not HEK-293T cells. These possibilities await

further testing using co-expression of these proteins combined with our FRET-based measurements.

Effects of the β_{1a} C-terminal Tail on DHPR Structure—In this study we have made the first direct FRET measurements between α_{1S} and β_{1a}. These measurements confirmed that both wild type and β_{1a}, bearing a 36-amino acid C-terminal truncation (β-36), bind to α_{1S} in our experimental system. In addition, relative to wild type β_{1a}, enhanced FRET was observed between the N termini of α_{1S} and the β-36 construct. This result suggests that this truncation results in a significant reorientation of β_{1a}, thereby bringing its N terminus closer to α_{1S}. Thus, deletion of the β_{1a} C terminus, which prevents bidirectional signaling (22, 23), also may affect the conformation/orientation of both the α_{1S} II-III loop and the β_{1a} subunit. These results are consistent with the hypothesis that the C terminus of the β_{1a} subunit is required for inducing conformational changes in the α_{1S} subunit necessary to transmit the EC coupling signal (20, 40).

Comparison with Recent High Resolution DHPR Structures—Recently, a near-atomic 4.2 Å resolution model of the DHPR complex has been published (18). Although many parts of the DHPR complex are well defined, none of the intracellular loops tested in this study are localized in the model, most likely due to high intrinsic flexibility of the loops. However, several aspects of the model support conclusions derived from our FRET data. For example, from this new cryo-EM reconstruction, it is evident that the II-III loop is the closest of the α_{1s} cytoplasmic loops (except the I-II loop) to the β_{1a} subunit (Fig. 7, *A* and *B*). Thus, it is conceivable that β_{1a} binding could modulate the structure of the II-III loop via short range allosteric interactions and that these two elements could form a structural complex. In addition, a central placement of the fused YFP would result in a relatively uniform profile of FRET efficiencies measured to the various intracellular loops (Fig. 7*A*). Indeed, the inherent intrinsic disorder of these loops revealed by the high resolution structures makes them excellent targets for further FRET-based structural studies to reveal subtle conformational changes underlying other important α_{1s} functionalities.

Author Contributions—M. M., C. F. P., and J. D. F. designed the study, executed the experiments, analyzed the results, and wrote the paper.

References

1. Beam, K. G., Knudson, C. M., and Powell, J. A. (1986) A lethal mutation in mice eliminates the slow calcium current in skeletal muscle cells. *Nature* **320,** 168–170
2. Beurg, M., Sukhareva, M., Strube, C., Powers, P. A., Gregg, R. G., and Coronado, R. (1997) Recovery of Ca^{2+} current, charge movements, and Ca^{2+} transients in myotubes deficient in dihydropyridine receptor β1 subunit transfected with β1 cDNA. *Biophys. J.* **73,** 807–818
3. Chaudhari, N., and Beam, K. G. (1989) The muscular dysgenesis mutation in mice leads to arrest of the genetic program for muscle differentiation. *Dev. Biol.* **133,** 456–467
4. Coronado, R., Ahern, C. A., Sheridan, D. C., Cheng, W., Carbonneau, L., and Bhattacharya, D. (2004) Functional equivalence of dihydropyridine receptor α_{1S} and β_{1a} subunits in triggering excitation-contraction coupling in skeletal muscle. *Biol. Res.* **37,** 565–575
5. Gregg, R. G., Messing, A., Strube, C., Beurg, M., Moss, R., Behan, M., Sukhareva, M., Haynes, S., Powell, J. A., Coronado, R., and Powers, P. A. (1996) Absence of the β subunit (cchb1) of the skeletal muscle dihydropyridine receptor alters expression of the α1 subunit and eliminates excitation-contraction coupling. *Proc. Natl. Acad. Sci. U.S.A.* **93,** 13961–13966
6. Knudson, C. M., Chaudhari, N., Sharp, A. H., Powell, J. A., Beam, K. G., and Campbell, K. P. (1989) Specific absence of the α1 subunit of the dihydropyridine receptor in mice with muscular dysgenesis. *J. Biol. Chem.* **264,** 1345–1348
7. Tanabe, T., Beam, K. G., Powell, J. A., and Numa, S. (1988) Restoration of excitation-contraction coupling and slow calcium current in dysgenic muscle by dihydropyridine receptor complementary DNA. *Nature* **336,** 134–139
8. Flucher, B. E., Obermair, G. J., Tuluc, P., Schredelseker, J., Kern, G., and Grabner, M. (2005) The role of auxiliary dihydropyridine receptor subunits in muscle. *J. Muscle Res. Cell Motil.* **26,** 1–6
9. Tanabe, T., Takeshima, H., Mikami, A., Flockerzi, V., Takahashi, H., Kangawa, K., Kojima, M., Matsuo, H., Hirose, T., and Numa, S. (1987) Primary structure of the receptor for calcium channel blockers from skeletal muscle. *Nature* **328,** 313–318
10. Catterall, W. A. (1988) Structure and function of voltage-sensitive ion channels. *Science* **242,** 50–61
11. Witcher, D. R., De Waard, M., Liu, H., Pragnell, M., and Campbell, K. P. (1995) Association of native Ca^{2+} channel β subunits with the α1 subunit interaction domain. *J. Biol. Chem.* **270,** 18088–18093
12. Pragnell, M., De Waard, M., Mori, Y., Tanabe, T., Snutch, T. P., and Campbell, K. P. (1994) Calcium channel β-subunit binds to a conserved motif in the I-II cytoplasmic linker of the α1-subunit. *Nature* **368,** 67–70
13. Grabner, M., Dirksen, R. T., Suda, N., and Beam, K. G. (1999) The II-III loop of the skeletal muscle dihydropyridine receptor is responsible for the Bi-directional coupling with the ryanodine receptor. *J. Biol. Chem.* **274,** 21913–21919
14. Nakai, J., Tanabe, T., Konno, T., Adams, B., and Beam, K. G. (1998) Localization in the II-III loop of the dihydropyridine receptor of a sequence critical for excitation-contraction coupling. *J. Biol. Chem.* **273,** 24983–24986
15. Weiss, R. G., O'Connell, K. M., Flucher, B. E., Allen, P. D., Grabner, M., and Dirksen, R. T. (2004) Functional analysis of the R1086H malignant hyperthermia mutation in the DHPR reveals an unexpected influence of the III-IV loop on skeletal muscle EC coupling. *Am. J. Physiol. Cell Physiol.* **287,** C1094–C1102
16. Peterson, B. Z., DeMaria, C. D., Adelman, J. P., and Yue, D. T. (1999) Calmodulin is the Ca^{2+} sensor for Ca^{2+}-dependent inactivation of L-type calcium channels. *Neuron* **22,** 549–558
17. Flucher, B. E., Kasielke, N., and Grabner, M. (2000) The triad targeting signal of the skeletal muscle calcium channel is localized in the COOH terminus of the α_{1S} subunit. *J. Cell Biol.* **151,** 467–478
18. Wu, J., Yan, Z., Li, Z., Yan, C., Lu, S., Dong, M., and Yan, N. (2015) Structure of the voltage-gated calcium channel Cav1.1 complex. *Science* **350,** aad2395
19. Karunasekara, Y., Dulhunty, A. F., and Casarotto, M. G. (2009) The voltage-gated calcium-channel β subunit: more than just an accessory. *Eur. Biophys. J.* **39,** 75–81
20. Schredelseker, J., Di Biase, V., Obermair, G. J., Felder, E. T., Flucher, B. E., Franzini-Armstrong, C., and Grabner, M. (2005) The β 1a subunit is essential for the assembly of dihydropyridine-receptor arrays in skeletal muscle. *Proc. Natl. Acad. Sci. U.S.A.* **102,** 17219–17224
21. Schredelseker, J., Dayal, A., Schwerte, T., Franzini-Armstrong, C., and Grabner, M. (2009) Proper restoration of excitation-contraction coupling in the dihydropyridine receptor β1-null zebrafish relaxed is an exclusive function of the β_{1a} subunit. *J. Biol. Chem.* **284,** 1242–1251
22. Eltit, J. M., Franzini-Armstrong, C., and Perez, C. F. (2014) Amino acid residues 489–503 of dihydropyridine receptor (DHPR) β_{1a} subunit are critical for structural communication between the skeletal muscle DHPR complex and type 1 ryanodine receptor. *J. Biol. Chem.* **289,** 36116–36124
23. Sheridan, D. C., Cheng, W., Ahern, C. A., Mortenson, L., Alsammarae, D., Vallejo, P., and Coronado, R. (2003) Truncation of the carboxyl terminus of the dihydropyridine receptor β_{1a} subunit promotes Ca^{2+} dependent

excitation-contraction coupling in skeletal myotubes. *Biophys. J.* **84,** 220–237
24. Papadopoulos, S., Leuranguer, V., Bannister, R. A., and Beam, K. G. (2004) Mapping sites of potential proximity between the dihydropyridine receptor and RyR1 in muscle using a cyan fluorescent protein-yellow fluorescent protein tandem as a fluorescence resonance energy transfer probe. *J. Biol. Chem.* **279,** 44046–44056
25. Polster, A., Ohrtman, J. D., Beam, K. G., and Papadopoulos, S. (2012) Fluorescence resonance energy transfer (FRET) indicates that association with the type I ryanodine receptor (RyR1) causes reorientation of multiple cytoplasmic domains of the dihydropyridine receptor (DHPR) α_{1S} subunit. *J. Biol. Chem.* **287,** 41560–41568
26. Raina, S. A., Tsai, J., Samsó, M., and Fessenden, J. D. (2012) FRET-based localization of fluorescent protein insertions within the ryanodine receptor type 1. *PLoS ONE* **7,** e38594
27. Adams, S. R., Campbell, R. E., Gross, L. A., Martin, B. R., Walkup, G. K., Yao, Y., Llopis, J., and Tsien, R. Y. (2002) New biarsenical ligands and tetracysteine motifs for protein labeling *in vitro* and *in vivo*: synthesis and biological applications. *J. Am. Chem. Soc.* **124,** 6063–6076
28. Griesbeck, O., Baird, G. S., Campbell, R. E., Zacharias, D. A., and Tsien, R. Y. (2001) Reducing the environmental sensitivity of yellow fluorescent protein: mechanism and applications. *J. Biol. Chem.* **276,** 29188–29194
29. Lee, D. Y., and Sugden, B. (2008) The LMP1 oncogene of EBV activates PERK and the unfolded protein response to drive its own synthesis. *Blood* **111,** 2280–2289
30. Chen, Y., Xue, S., Zou, J., Lopez, J. R., Yang, J. J., and Perez, C. F. (2014) Myoplasmic resting Ca^{2+} regulation by ryanodine receptors is under the control of a novel Ca^{2+}-binding region of the receptor. *Biochem. J.* **460,** 261–271
31. Fessenden, J. D. (2009) Förster resonance energy transfer measurements of ryanodine receptor type 1 structure using a novel site-specific labeling method. *PLoS ONE* **4,** e7338
32. Mahalingam, M., and Fessenden, J. D. (2015) Methods for labeling skeletal muscle ion channels site-specifically with fluorophores suitable for FRET-based structural analysis. *Methods Enzymol.* **556,** 455–474
33. Girgenrath, T., Mahalingam, M., Svensson, B., Nitu, F. R., Cornea, R. L., and Fessenden, J. D. (2013) N-terminal and central segments of the type 1 ryanodine receptor mediate its interaction with FK506-binding proteins. *J. Biol. Chem.* **288,** 16073–16084
34. Fessenden, J. D., and Mahalingam, M. (2013) Site-specific labeling of the type 1 ryanodine receptor using biarsenical fluorophores targeted to engineered tetracysteine motifs. *PLoS ONE* **8,** e64686
35. Pettersen, E. F., Goddard, T. D., Huang, C. C., Couch, G. S., Greenblatt, D. M., Meng, E. C., and Ferrin, T. E. (2004) UCSF Chimera: a visualization system for exploratory research and analysis. *J. Comput. Chem.* **25,** 1605–1612
36. Flucher, B. E., Andrews, S. B., and Daniels, M. P. (1994) Molecular organization of transverse tubule/sarcoplasmic reticulum junctions during development of excitation-contraction coupling in skeletal muscle. *Mol. Biol. Cell* **5,** 1105–1118
37. Bannister, R. A., Grabner, M., and Beam, K. G. (2008) The α_{1S} III-IV loop influences 1,4-dihydropyridine receptor gating but is not directly involved in excitation-contraction coupling interactions with the type 1 ryanodine receptor. *J. Biol. Chem.* **283,** 23217–23223
38. Stroffekova, K., Proenza, C., and Beam, K. G. (2001) The protein-labeling reagent FLASH-EDT2 binds not only to CC*XX*CC motifs but also non-specifically to endogenous cysteine-rich proteins. *Pflugers Arch.* **442,** 859–866
39. Griffin, B. A., Adams, S. R., Jones, J., and Tsien, R. Y. (2000) Fluorescent labeling of recombinant proteins in living cells with FlAsH. *Methods Enzymol.* **327,** 565–578
40. Dayal, A., Bhat, V., Franzini-Armstrong, C., and Grabner, M. (2013) Domain cooperativity in the β_{1a} subunit is essential for dihydropyridine receptor voltage sensing in skeletal muscle. *Proc. Natl. Acad. Sci. U.S.A.* **110,** 7488–7493
41. Bannister, R. A., Papadopoulos, S., Haarmann, C. S., and Beam, K. G. (2009) Effects of inserting fluorescent proteins into the α_{1S} II-III loop: insights into excitation-contraction coupling. *J. Gen. Physiol.* **134,** 35–51
42. Hulme, J. T., Konoki, K., Lin, T. W.-C., Gritsenko, M. A., Camp, D. G., 2nd, Bigelow, D. J., and Catterall, W. A. (2005) Sites of proteolytic processing and noncovalent association of the distal C-terminal domain of CaV1.1 channels in skeletal muscle. *Proc. Natl. Acad. Sci. U.S.A.* **102,** 5274–5279
43. Deleted in proof
44. Proenza, C. (2000) Excitation-contraction coupling is not affected by scrambled sequence in residues 681–690 of the dihydropyridine receptor II-III loop. *J. Biol. Chem.* **275,** 29935–29937
45. Flucher, B. E., Kasielke, N., Gerster, U., Neuhuber, B., and Grabner, M. (2000) Insertion of the full-length calcium channel α_{1S} subunit into triads of skeletal muscle *in vitro*. *FEBS Lett.* **474,** 93–98